

Computer simulation of the structural transformation in liquid Al_2O_3

This article has been downloaded from IOPscience. Please scroll down to see the full text article.

2005 J. Phys.: Condens. Matter 17 3025

(<http://iopscience.iop.org/0953-8984/17/19/016>)

View [the table of contents for this issue](#), or go to the [journal homepage](#) for more

Download details:

IP Address: 129.252.86.83

The article was downloaded on 27/05/2010 at 20:44

Please note that [terms and conditions apply](#).

Computer simulation of the structural transformation in liquid Al_2O_3

Vo Van Hoang¹ and Suhk Kun Oh²

¹ Department of Physics, College of Natural Sciences, HochiMinh City National University, 227 Nguyen Van Cu Street, District 5, HochiMinh City, Vietnam

² Department of Physics, Chungbuk National University, Cheongju 361-763, Korea

E-mail: vhoang2002@yahoo.com

Received 10 March 2005, in final form 4 April 2005

Published 29 April 2005

Online at stacks.iop.org/JPhysCM/17/3025

Abstract

We investigate the pressure-induced structural transformation in liquid Al_2O_3 by a molecular dynamics (MD) method. Simulations were done in the basic cube, under periodic boundary conditions, containing 3000 ions with Born–Mayer-type pair potentials. The structure of the liquid Al_2O_3 model with a real density at ambient pressure is in good agreement with Landron’s experiment. In order to study the structural transformation, seven models of liquid alumina at temperature 2500 K and at densities in the range 2.80–4.5 g cm⁻³ have been built. The microstructure of Al_2O_3 systems has been analysed through the pair radial distribution functions, coordination number distributions, interatomic distances and bond-angle distributions. And we found clear evidence of a structural transition in liquid alumina from a tetrahedral to an octahedral network. According to our results, this transformation occurred at densities in the range 3.6–4.5 g cm⁻³. We also obtained an anomalous density dependence of the self-diffusion constant in the region of the structural transformation.

1. Introduction

In the Earth’s interior, silicate and alumino-silicate melts change their local structure causing strong density and viscosity modifications in magmas [1], and silicon exhibits at high pressure a change of its coordination number [2]. These results have been mostly obtained in high pressure–temperature experiments [3] but also in computer simulations [4–8]. Gutierrez investigated the pressure-induced structural transformation in Al_2O_3 glass using a MD method [5]; the simulations were done on five systems containing 1800 ions at densities in the range 3.175–4.2 g cm⁻³ with Matsui’s pair potential [5]. Calculations showed that as the density increases from 3.175 to 4.2 g cm⁻³ the Al–O bond length increases and other bond lengths, O–O and Al–Al, decrease. The peak of the Al–O coordination number changes from 4 to 6 and the O–Al–O bond angle changes from 105° to 90°. This result is confirming evidence

of a structural transformation from a tetrahedral to an octahedral network. This phenomenon was called the amorphous–amorphous phase transition in glasses. Phase transitions of minerals under pressure govern several geophysical properties of the Earth, where silicates and aluminosilicates play a key role. Therefore, detailed knowledge of the structure of silica and alumina in the liquid and amorphous states, and their behaviour under large applied pressure, is essential to understanding the flow of magma. On the other hand, in the case of water and silica, it has been proposed that the polymorphism of the amorphous solids may be due to a trend towards a liquid–liquid phase separation [9–11] and, indeed, recent simulations seem to confirm this hypothesis [12–14]. In order to make a theoretical study of this phenomenon, it is necessary to have a reliable model of the liquid as well as a complete characterization of it, from both the structural and dynamic points of view. However, while there are several experimental and theoretical studies for liquid silica [15], and recently for liquid germania [4, 16], we have not found any study regarding pressure-induced structural transformation in liquid alumina. Furthermore, most of the previous studies, concerning structural transformations in liquid or amorphous oxides, mainly concentrated on the structural aspect of the problem. In this work, we will study the structural transformation in liquid alumina by means of computer simulation to provide additional understanding of the transition. This paper is organized as follows. In section 2 we describe the calculation method and the preparation of the liquid state. Results and discussion of the structural and dynamical changes are presented in section 3. Conclusions will be given in section 4.

2. Calculation

Liquid Al_2O_3 models containing 3000 ions in a basic cube with periodic boundary conditions were constructed by the MD method at densities ranging from 2.80 to 4.50 g cm^{-3} . The Born–Mayer-type pair potential used here is of the form

$$u_{ij}(r) = z_i z_j \frac{e^2}{r} + B_{ij} \exp\left(-\frac{r}{R_{ij}}\right) \quad (1)$$

where the terms represent Coulomb, repulsion and van der Waals energies, respectively. Parameter r is the distance between the centres of the i th and j th ions; z_i and z_j are the charges of the i th and j th ions; B_{ij} and R_{ij} are the parameters accounting for the repulsion of the ionic shells. The values $z_1 = +3$ and $z_2 = -2$ are the charges of Al^{3+} and O^{2-} . The values $B_{11} = 0$, $B_{12} = 1779.86$ eV, $B_{22} = 1500$ eV and $R_{ij} = 29$ pm and details about the potentials and calculation method can be found in [17]. Using such potentials we have successfully simulated the structure and properties of liquid and amorphous Al_2O_3 [17, 18]. The equilibrium liquid model with a real density at ambient pressure ($\rho = 2.80$ g cm^{-3}) at temperature 2500 K was reached after 50 000 MD time steps by ‘heating up’ the initial amorphous Al_2O_3 model previously obtained at temperature 2000 K in [17]. Moreover, in order to obtain liquid models at different densities upon compression, the volume of the basic simulation cube is reduced isotropically in corresponding steps. After each volume change, the system is thermalized for 50 000 MD steps to reach an equilibrium amorphous state at constant density (e.g. at constant volume) and at a fixed temperature of 2500 K. We have calculated structural and dynamical characteristics of the models obtained.

The molecular dynamics methods involve calculations of trajectories of particles under the action of the forces from neighbouring particles in the model. For the MD method we used the Verlet algorithm with a time step $\Delta t = 4.0749 \times 10^{-16}$ s. In order to calculate coordination number distributions and bond-angle distributions in the liquid Al_2O_3 we adopt the fixed values $R_{\text{Al–Al}} = 3.7$ Å, $R_{\text{Al–O}} = 2.2$ Å and $R_{\text{O–O}} = 3.3$ Å. Here R is a cut-off

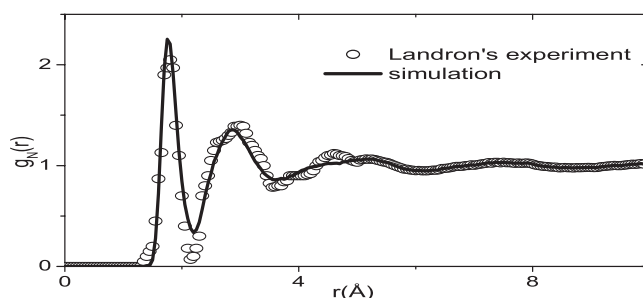


Figure 1. Total neutron radial distribution function of liquid Al₂O₃ model at the temperature of 2500 K and at the density of 2.80 g cm⁻³ and experimental data given in [19].

Table 1. Some characteristics of liquid Al₂O₃ at different densities. r_{ij} —positions of the first peaks in the partial radial distribution functions (PRDFs) $g_{ij}(r)$; g_{ij} —the heights of the first peaks in PRDFs; Z_{ij} —the average coordination number (1–1 for the Al–Al pair, 1–2 for the Al–O pair, 2–1 for the O–Al pair, 2–2 for the O–O pair); p —the mean pressure in model; E —the mean total energy of the model.

Density (g cm ⁻³)	p (GPa)	$-E$ (10 ⁴ eV)	r_{ij} (Å)			g_{ij}			Z_{ij}			
			1–1	1–2	2–2	1–1	1–2	2–2	1–1	1–2	2–1	2–2
2.80	0.05	9.160	3.20	1.77	2.80	2.79	5.67	2.23	8.00	4.20	2.80	7.44
			^a 3.25	1.78	2.84	1.70	5.60	2.40		4.20		
3.09	4.31	9.166	^b 3.15	1.75	2.75	1.90	5.30	2.50	8.24	4.10	2.72	8.84
			3.15	1.78	2.72	2.83	5.16	2.27	9.07	4.38	2.92	8.36
3.30	11.0	9.167	3.11	1.79	2.65	2.83	4.83	2.35	9.95	4.51	3.01	9.10
3.60	25.6	9.156	3.03	1.79	2.58	2.89	4.71	2.50	10.9	4.80	3.19	9.91
3.90	48.0	9.123	2.95	1.79	2.52	2.92	4.70	2.66	11.5	5.12	3.41	10.5
4.20	78.2	9.066	2.88	1.77	2.46	2.99	4.74	2.73	12.2	5.41	3.61	11.0
4.50	114.5	8.982	2.82	1.76	2.40	3.01	4.73	2.82	12.5	5.70	3.80	11.3

^a Experimental data at ambient pressure given in [20, 21].

^b Calculated data at ambient pressure given in [22].

radius, which was chosen as the position of the minimum after the first peak in $g_{ij}(r)$ for the liquid model at ambient pressure.

3. Results and discussion

3.1. Structural characteristics of liquid Al₂O₃

Table 1 and figure 1 show structural characteristics of the Al₂O₃ at the real density of 2.80 g cm⁻³ in our simulations, and they are close to the experiment data of [19–21] and to the calculated data given in [22]. The PRDFs agree with calculated PRDFs in [22] in terms of the shape, position and amplitude of the peaks. We also display the calculated total neutron-weighted pair distribution function $g_N(r)$ for liquid Al₂O₃ (details about the calculation of $g_N(r)$ can be seen in [17]). Figure 1 shows that our calculated $g_N(r)$ is close to the experimental one obtained by Landron *et al* [19] and with calculated data given in [22]. As presented in [20, 21], liquid Al₂O₃ at ambient pressure has the structure of a tetrahedral network with the average coordination number $Z_{Al-O} \sim 4$. The structural element of the network is a slightly distorted (AlO₄)⁵⁻ tetrahedron. The same structure also exists in our

Table 2. Coordination number distribution for the pair, $Z_{\text{Al-O}}$, in the liquid state at different densities.

$Z_{\text{Al-O}}$	3	4	5	6	7	8
Number of Al^{3+} ions ($\rho = 2.80 \text{ g cm}^{-3}$)	98	785	303	14	0	0
Number of Al^{3+} ions ($\rho = 3.09 \text{ g cm}^{-3}$)	68	646	448	37	0	0
Number of Al^{3+} ions ($\rho = 3.30 \text{ g cm}^{-3}$)	61	533	539	67	0	0
Number of Al^{3+} ions ($\rho = 3.60 \text{ g cm}^{-3}$)	24	385	612	179	0	0
Number of Al^{3+} ions ($\rho = 3.90 \text{ g cm}^{-3}$)	11	189	649	344	7	0
Number of Al^{3+} ions ($\rho = 4.20 \text{ g cm}^{-3}$)	5	97	528	537	32	1
Number of Al^{3+} ions ($\rho = 4.50 \text{ g cm}^{-3}$)	0	45	385	663	102	5

model at the density of 2.80 g cm^{-3} (see table 1). We can see tetrahedral network structure of the liquid Al_2O_3 model at the same density through the coordination number distribution of aluminium ions for the pair Al–O (table 2). As shown in table 2, Al atoms are mainly surrounded by four oxygen atoms.

Table 1 shows that as the density increases from 2.80 to 4.5 g cm^{-3} , the Al–O bond length slightly increases and then decreases and it differs somewhat from Gutierrez's results for the case of amorphous Al_2O_3 [5], where it was found that the Al–O bond length increases with density, and this is possibly related to the different potentials used here and in [5]. Other bond lengths decrease with density as in amorphous states [5]. The height of the first peak, g_{ij} , in the radial distribution function for the pair Al–O decreases with density, but for other pairs it increases. Mean coordination numbers for all pairs of atoms increase with density. This means that, when the density increases, not only does the size of the structural units decrease, but also the length of the connection between them decreases, indicating a close packed-like structure. Note that from an experimental point of view the coordination number, and therefore the proportion of different polyhedra, appears to be related to the density of the samples. It is clear from table 2 that in the simulated Al_2O_3 , the number of overcoordinated polyhedra (AlO_6 , AlO_7 , AlO_8) increases as the number of the less coordinated units (AlO_3 , AlO_4) decreases with the density. The number of AlO_5 polyhedra increases and then decreases. In particular, the mean coordination number for the pair Al–O ($Z_{\text{Al-O}}$; see table 1) changes from 4.20 at low density to 5.70 at high density. Therefore, we found the same behaviour as reported in experiments and this is related to the structural transformation in liquid alumina, where the structure changes from a tetrahedral to an octahedral network. This is similar to the cases observed for other tetrahedral network, such as amorphous silica [23] and germania [24, 25]. This structural transformation occurs at densities between 3.6 and 4.2 g cm^{-3} according to our calculations for liquid alumina.

Figure 2 shows the MD results for the total and partial pair distribution functions $g_{ij}(r)$ at three different densities. As the density increases, the Al–Al first peak shifts to the left but without splitting into two peaks as found for the amorphous states [5]. At distances beyond the nearest neighbours, there are many more peaks in the total RDF and in PRDF for the pair O–O at high density compared to low density, a fact indicating a close packed-like structure.

More details about the local atomic rearrangement with density can be seen in figure 3, which presents the coordination number distributions in the liquid models at three densities. We can find clear evidence of a structural transformation from a tetrahedral to an octahedral network when the density increases through the coordination number for the pair Al–O. At the density of 4.5 g cm^{-3} such a distribution has a sharp peak at the value 6.

Further information about the local structure is provided by the bond-angle distributions. We do not account for all bond-angle distributions, but the most important of them are the

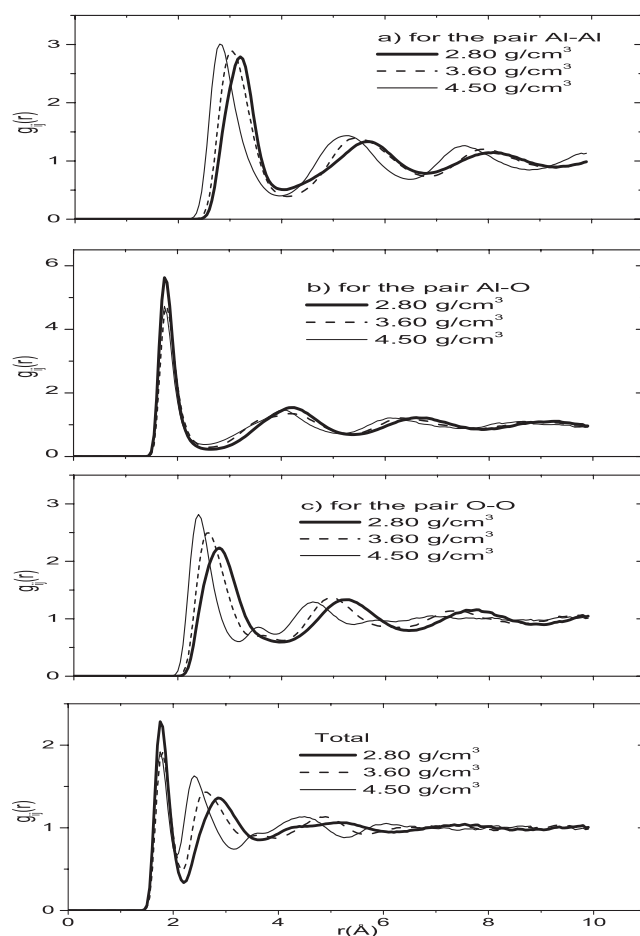


Figure 2. Pair distribution functions of liquid Al_2O_3 models at three different densities.

O–Al–O and Al–O–Al bond-angle distributions presented in figure 4. We display the angle distributions calculated with Al–Al, Al–O and O–O cut-off distances of 3.70, 2.20 and 3.20 Å, respectively. From the coordination number distributions we infer that at low density the basic units are tetrahedral AlO_4 . From figure 4(a), it can be seen that, at low density, the O–Al–O bond-angle distribution has a peak at 102° and the peak moves toward smaller values when the density increases. At the density of 4.50 g cm^{-3} the peak is somewhere around 80° ; this value is consistent with the changes in the interatomic distances and coordination numbers, the basic units becoming an octahedron and other highly coordinated units (AlO_5 , AlO_7). A similar change in the O–Al–O bond-angle distribution with density has been obtained in amorphous Al_2O_3 models [5].

The Al–O–Al bond angle can be used to describe the connectivity of the structural units. As shown in figure 4(b), at low density the Al–O–Al bond-angle distribution has a peak at 115° and it moves toward smaller values as the density increases. At the density of 4.50 g cm^{-3} the peak is centred on 95° . The same tendency has been found for amorphous states in [5] and, because this bond-angle distribution can be used to describe the connectivity between structural units AlO_x , we can infer that at low densities tetrahedra are linked to each other mainly in two

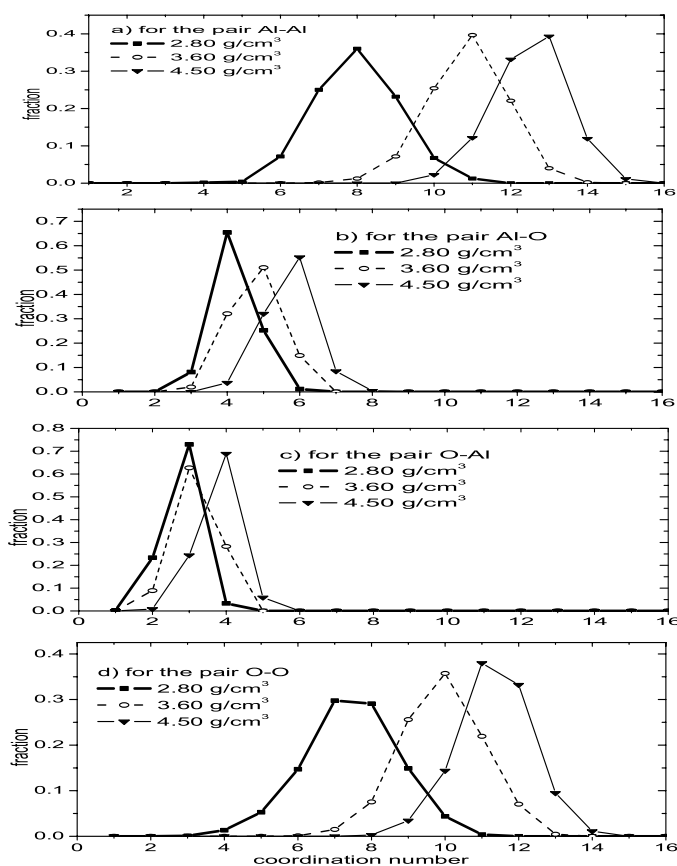


Figure 3. Coordination number distribution in liquid Al_2O_3 models at three densities.

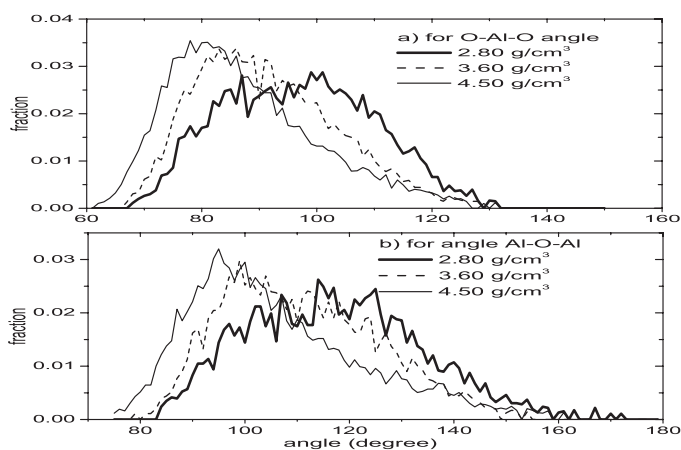


Figure 4. The bond-angle distributions in liquid Al_2O_3 models at three densities.

ways: edge-sharing tetrahedral and corner-sharing tetrahedral. When the density increases, the system changes from a mainly corner-sharing tetrahedral network at low density to a network

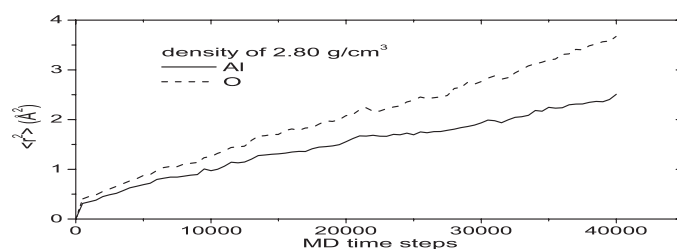


Figure 5. Mean squared displacements of Al and O ions in the liquid Al₂O₃ model at the density of 2.80 g cm⁻³.

which contains mostly octahedra as a basic unit, linked to each other by sharing edges and/or faces as in amorphous Al₂O₃ models [5].

3.2. Self-diffusion in liquid Al₂O₃ models during the pressure-induced structural transformation

When people investigate the structural transformation in liquids, they often study only a structural aspect of the problem; we considered this a serious shortcoming. In this work, the dynamical changes during pressure-induced structural transformation in liquid Al₂O₃ will be studied in detail, as presented below.

If the interparticle potential is known, it is easy to calculate the self-diffusion constants of a liquid by a molecular dynamics method. In the process of molecular dynamics relaxation of the liquid phase, the particles of the model at each temporal step perform small displacements correlated with displacements of neighbouring particles. Hence, the cooperative diffusion mechanism is realized. The self-diffusion constants of ions in the liquid Al₂O₃ model can be determined through the mean squared particle displacement $\langle r^2 \rangle$ via the Einstein relation:

$$D = \lim_{t \rightarrow \infty} \frac{\langle r^2(t) \rangle}{6t}. \quad (2)$$

Liquid Al₂O₃ models at $T = 2500$ K can be obtained by ‘heating up’ the 2000 K amorphous Al₂O₃ model through a long MD relaxation (after 50 000 MD time steps) to reach a good equilibrium liquid state for calculating structural properties. However, after the first 10 000 MD steps when the system is reaching a quasi-equilibrium state at each density, we can begin determining the mean square particle displacement $\langle r^2 \rangle$ for calculating diffusion constants D in another 40 000 MD time steps. The time dependence of $\langle r^2 \rangle$ is presented in figure 5.

The density dependence of the diffusion constant is presented in figure 6. We can see that the diffusion constant for both ions Al and O decreases with density in the first stage and then it increases. Usually, when models of dense noncrystalline systems with short range pair potentials (argon and metals) are considered, pressure enhancement often results in a decrease of the self-diffusion constant. Other situations may also emerge, however. For the case of the pair Gauss potential $u(r) = u_o \exp(-br^2)$, Stillinger and Weber also discovered an anomalous increase of the self-diffusion constant on compression of the system. This effect emerges because as the distance decreases, the force function $-du(r)/dr$ passes through a maximum and then decreases, too. Another example of anomalous behaviour is presented by loose structures of the silica type, where the structure changes under pressure, the coordination numbers grow and three-body contributions to the potential begin to play a smaller role. For instance, in the MD modelling of silica in the ionic model at 1400 K, a rise in pressure up to

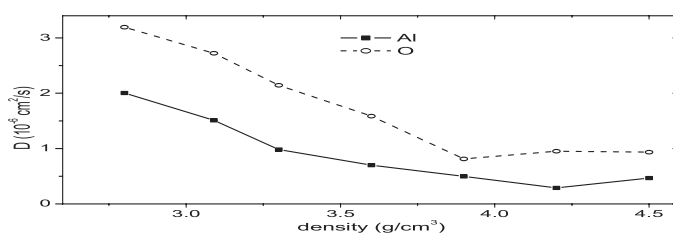


Figure 6. The density dependence of the diffusion constant.

12 GPa leading to a severalfold increase in the ion self-diffusion constant, and under a further increase of pressure up to 36 GPa, these constants slowly decreased [26]. The enhancement of the ionic mobility in MD models of liquid silica under pressure was also studied by Tsuneyuki and Matsui [27] and they explained the anomalous diffusion properties of liquid silica under pressure on the basis of a pressure-induced structural transformation in silica. The anomalous diffusion in our alumina system can be explained by the same way. Figure 6 shows that an anomalous increase in the diffusion constant occurred at a density of more than 3.60 g cm^{-3} , where the structure of the system is transforming from a tetrahedral to an octahedral network (see table 2) and it may be related to the new diffusion mechanism in the new structural phase of liquid alumina.

The nature of the pressure-induced structural transformation is not firmly established due to the scarcity of experiments at the extreme conditions at which the structural transitions take place [28]. The majority of the evidence suggests that it is a first-order transition, i.e., it entails discontinuities in density and enthalpy [29]. However, the statement can be found in [30] that, generally, such transitions are higher than first order, and structural changes are not accompanied by volume and enthalpy discontinuities except in a few cases. There is no direct experimental evidence of a pressure-induced structural transformation in liquid alumina; however, the coexistence of two liquid phases with the same composition but different densities has been observed in a supercooled melt of $\text{Al}_2\text{O}_3\text{--Y}_2\text{O}_3$ (see [31]). It seems that the structural transformation in liquid Al_2O_3 upon compression at the temperature of 2500 K was gradual and continuous, like those observed in several other materials [30].³ Moreover, this structural transformation was also accompanied by anomalous diffusion as previously obtained for liquid SiO_2 (see figure 6 and [27]).

4. Conclusions

The structure of the liquid Al_2O_3 model with a real density at ambient pressure, constructed by a MD method using an ionic model with Born–Mayer-type pair potentials, is in good agreement with experimental data. Calculations showed that in the liquid state there is a short range order dominated by a slightly distorted $(\text{AlO}_4)^{5-}$ tetrahedron. Calculated self-diffusion constants for Al^{3+} and O^{2-} in liquid Al_2O_3 have reasonable values. Our calculations revealed that, when the density of the liquid alumina model increased from 2.80 to 4.50 g cm^{-3} , the pressure-induced structural transformation could occur anywhere in the range $3.60\text{--}4.50 \text{ g cm}^{-3}$ and we found clear evidence for a structural transformation from a tetrahedral to an octahedral network. We

³ We need to test the density dependence of the enthalpy and $P\text{--}V$ isotherm of the system and clear evidence of a first-order phase transition has not been found (no abrupt transition from a tetrahedral to an octahedral network structure) due to the existence of the fivefold-coordinated unit AlO_5 in the system; more details can be seen in our subsequent work in this direction, which will be published elsewhere.

also found an anomalous density dependence of the self-diffusion constant in the region of the structural transformation.

Acknowledgments

This work was supported by the Korean Science and Engineering Foundation (KOSEF) and it was accomplished at the Department of Physics, Chungbuk National University, Cheongju, South Korea.

References

- [1] Brueckner R 1970 *J. Non-Cryst. Solids* **5** 123
- [2] Hemley R J, Mao H K, Bell P M and Mysen B O 1986 *Phys. Rev. Lett.* **57** 747
- [3] Williams Q and Jeanloz R 1988 *Science* **239** 902
- [4] Gutiérrez G and Rogan J 2004 *Phys. Rev. E* **69** 031201
- [5] Gutierrez G 2002 *Rev. Mex. Fis.* **48** (S3) 60
- [6] Guissani Y and Guillot B 1996 *J. Chem. Phys.* **104** 7633
- [7] Micoulaut M 2004 *J. Phys.: Condens. Matter* **16** L131
- [8] Tse J S, Klug D D and LePage Y 1992 *Phys. Rev. B* **46** 5933
- [9] Poole P H, Sciortino F, Essmann U and Stanley H E 1992 *Nature* **360** 324
- [10] Poole P H, Hemmati M and Angell C A 1997 *Phys. Rev. Lett.* **79** 2281
- [11] Lacks D J 2000 *Phys. Rev. Lett.* **84** 4629
- [12] Roberts C J, Panagiotopoulos A Z and Debenedetti P G 1996 *Phys. Rev. Lett.* **77** 4386
- [13] Harrington S, Zhang R, Poole P H, Sciortino F and Stanley H E 1997 *Phys. Rev. Lett.* **78** 2409
- [14] Saika-Voivod I, Sciortino F and Poole P H 2000 *Phys. Rev. E* **63** 011202
- [15] Trave A, Tangney P, Scandolo S, Pasquarello A and Car R 2002 *Phys. Rev. Lett.* **89** 245504
- [16] Meyer A, Schober H and Neuhaus J 2001 *Phys. Rev. B* **63** 212202
- [17] Hoang V V 2004 *Phys. Rev. B* **70** 134204
- [18] Hoang V V and Oh S K 2004 *Phys. Rev. E* **70** 061203
- [19] Landron C, Soper A K, Jenkins T E, Greaves G N, Hennem L and Coutures J P 2001 *J. Non-Cryst. Solids* **293–295** 453
- [20] Landron C, Hennem L, Jenkins T E, Greaves G N, Coutures J P and Soper A K 2001 *Phys. Rev. Lett.* **86** 4839
- [21] Greaves G N, Jenkins T, Soper A, Landron C, Hennem L and Coutures J P available at <http://www.estec.esa.nl/conferences/00a06/abstracts/223.html>
- [22] Gutiérrez G, Belonoshko A B, Ahuja R and Johansson B 2000 *Phys. Rev. E* **61** 2723
- [23] Grimsditch M 1984 *Phys. Rev. Lett.* **52** 2379
- [24] Itie J P, Polian A, Calas G, Petiau J, Fontaine A and Tolentino H 1989 *Phys. Rev. Lett.* **63** 398
- [25] Smith K H, Shero E, Chizmesnya A and Wolf G H 1995 *J. Chem. Phys.* **102** 6851
- [26] Tsuneyuki S 1992 *Molecular Dynamics Simulations (Springer Series in Solid-State Sciences vol 103)* ed F Yonezawa (Berlin: Springer)
- [27] Tsuneyuki S and Matsui Y 1995 *Phys. Rev. Lett.* **74** 3197
- [28] Huang L and Kieffer J 2004 *Phys. Rev. B* **69** 224203
- [29] Shell M S, Debenedetti P G and Panagiotopoulos A Z 2002 *Phys. Rev. E* **66** 011202
- [30] Roberts C J, Panagiotopoulos A Z and Debenedetti P G 1996 *Phys. Rev. Lett.* **77** 4386
- [31] Aasland S and McMillan P F 1994 *Nature* **369** 633